IRRMA 6, held 20.-24.6.2005 at McMaster University in Hamilton, Ontario, Canada
Paper #106

AIRBORNE GAMMA SURVEY IN SNOW MASS DETERMINATION

S.S.H. Kasi [1]
Helsinki University of Technology

Abstract

In the airborne measurement of soil gamma radiation the snow cover causes intensity attenuation. The photon energy peaks of detector spectra are symmetric due to, that the most of small-angle scatterings are not Compton scatterings, but Rayleigh scatterings. Mathematics to calculate the energy peak counting rates is presented. Because of GPS, today the airborne route can be flown and repeated accurately.

92.20.Td , 92.40.Rm, 29.30.Kv
Soil radioactivity, gamma attenuation, snow water equivalent

1. Introduction

The airborne measurement of gamma photons emitted by radioactive elements of the earth has been during decades applied [1,2]. As a detector the scintillation spectrometer NaI(Tl) is used a lot. Its energy resolution is mostly sufficient. The photopeaks of the most significant natural gamma photons (1461 keV of ^{40}K, 1765 keV of ^{214}Bi and 2614 keV of ^{208}Tl) are clearly separated. Pure germanium photodiodes (HPGe) have better resolutions. More dense materials with the same resolution have recently been developed. The detector, its electronic system and data registration equipments can be flown in vehicles as airplane and helicopter.

The natural gamma radiation have been used for determination of the water equivalent of snow cover in North America [3,4] and Eurasia, in Finland [5] not in this century.

In Europe the 1986 Chernobyl deposition of the ^{137}Cs (half-live 30.07 a) is significant today. ^{137}Cs emits only a gamma photon having so low energy as 661.6 keV.

[1] Servo Kasi
Kajavankatu 6 B 45
FI-04230 Kerava, Finland

fax +358 9 2428550, if on, tel. +358 9 2428550, +358 50 5724009
email servo.kasi@helsinki.fi

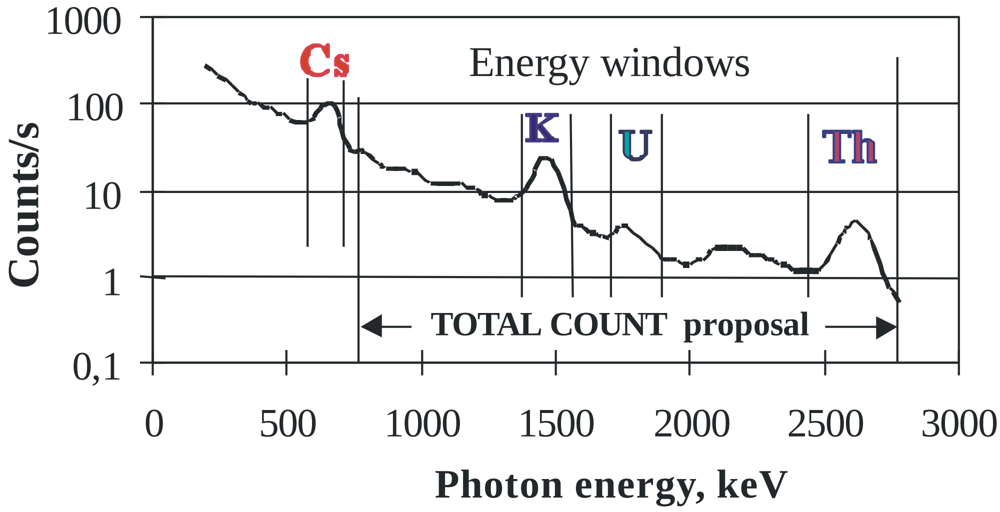

Fig. 1. Airborne scintillation spectrum in Finland in 2000 (the permission of Geophysical Survey of Finland). Author's proposal [22] for the TOTAL COUNT window because of Cs-deposition.

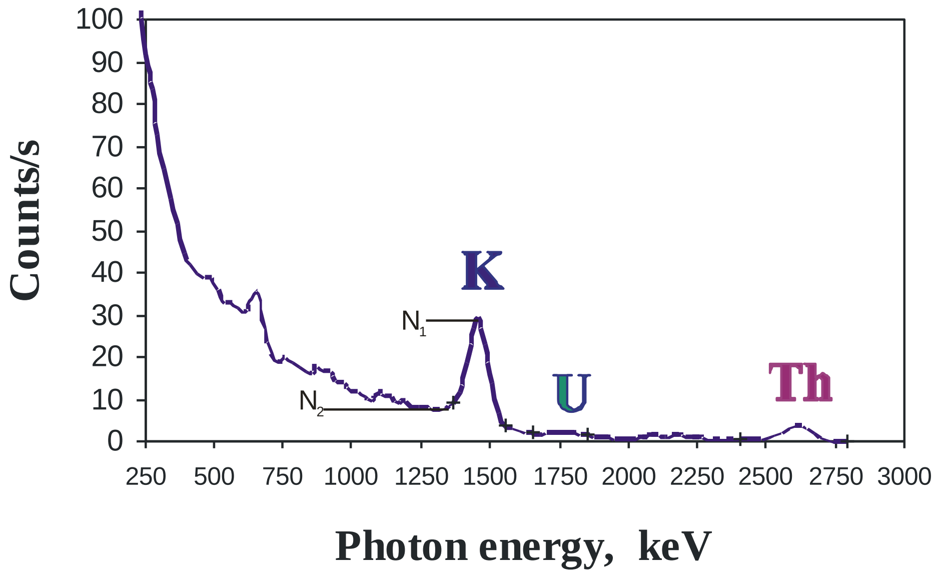

Fig. 2. Airborne scintillation spectrum in Finland before 1986 (the permission of Geophysical Survey of Finland).

2. Gamma spectra characteristics

In the airborne spectra the peak of potassium isotope ^{40}K at 1.461 MeV is called K-window, that of ^{214}Bi at 1.765 MeV U-window, and that of ^{208}Tl at 2.614 MeV Th-window, Fig. 1 and 2. In Fig. 1 the peak caused by ^{137}Cs-photons (662 keV) is clear. ^{214}Bi and ^{208}Tl emit also smaller energy photons [1,6].

Why in the spectra the gamma peaks are so symmetric? In the scintillation and pure germanium spectra (an excample, Fig. 3) you do not see the signs of remarkable small-energy-change Compton scatterings, though the Klein-Nishina Compton-scattering cross section

$$\frac{d\sigma_{KN}}{d\Omega} = \frac{1}{2} r_0^2 \left(\frac{k_2}{k_1}\right)^2 \left(\frac{k_2}{k_1} + \frac{k_1}{k_2} - \sin^2\theta\right) \qquad (1)$$

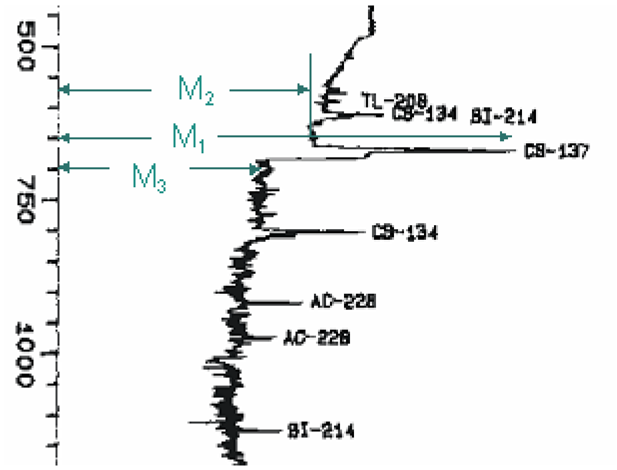

Fig. 3. The energies 450 – 1180 keV part of a French HPGe-spectrum in RESUME 1995 [21] in Finland.

has a maximum at the scattering angle $\theta = 0$. k_1 is the wave number before and k_2 after the scattering. However, many investigations, e.g. [7,8] show

$$\frac{d\sigma_C}{d\Omega} = \frac{d\sigma_{KN}}{d\Omega} S(x,Z), \qquad (2)$$

where $x = \sin(\theta/2)/\lambda$, λ is the initial photon wave length ($k_1 = 2\pi/\lambda$), Z means an element and $S \in [0,1]$. When the scattering angle is zero, then $x = 0$. The investigations show $S(0,Z) = 0$ for all elements, even metals. To use the function $S(E,\theta,Z)$ instead of $S(x,Z)$, when E is the energy of a photon colliding with the element, it has not been seen necessary, yet recently [9,10]. The compilation of $S(x,Z)$ used here is in [11].

Maybe a big part of the counting rate N_2 in Fig. 2 is caused by relatively small angle Compton scatterings of K-photons. The low angle-region, where S is needed, increases with Z, but decreases when E increases: Cs $\rightarrow$ K $\rightarrow$ U $\rightarrow$ Th in Fig. 4.

Fig. 4. Angles of $S(x,Z) = 0.99$, $x = \sin(\theta/2)/\lambda$, for Cs-, K-, U- and Th-photons.

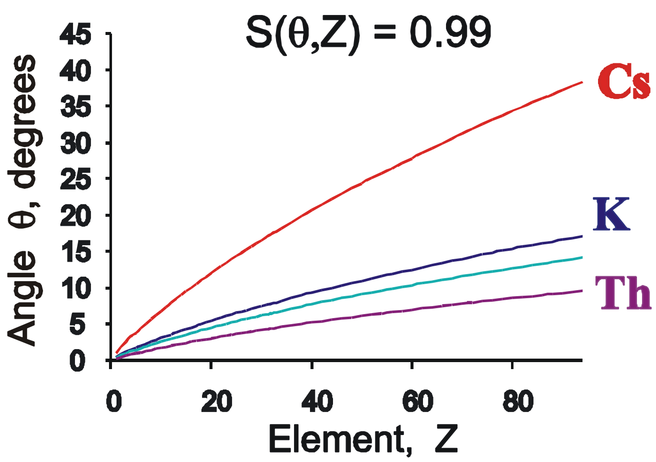

2.1. Energy-retaining scatterings contribution in photopeaks

Rayleigh scattering, nuclear Thompson and Delbrück scatterings are such that in them the photon colliding with an atom retains its intial energy. Below photon energy 3 MeV only these three such scatterings are significant. Fig. 5 illustrates the airborne measurement. There have been drawn two rays travelling straightly from soil into the detector.

The differential Rayleigh scattering cross section (DRC) for the energy 300 keV photon [12, Fig. 2.2] on carbon atom at 15° is about 3000 times smaller than its value calculated to 0° and on lead atom almost 200 times smaller than at θ = 0°. For the 300 keV photon and for the scattering θ = 15° we have x = 3.16 and then the form factor [11] $F(x, Z) < 10^{-4}$ for Z = 1, and $F(0, 1) = 1$. The corresponding Thompson cross sections are almost equal and for DRC they are multiplied by the square of F, [13]. For the other elements the changes in the phenomenum between hydrogen and carbon and carbon and lead are monotonous.

The Delbrück scattering has small cross section, and it is clearly directed forward [14, and its references] at these "low energies". The cross section of nuclear Thompson scattering is even smaller [10,15].

Rayleigh scattering cross section and other energy-retaining cross sections shall not be included in the total scattering cross section, when the photon attenuations are calculated at the energies below 3 MeV. Large angle part of those scatterings only insignificantly increases the emitter density in soil.

3. Soil gamma measuring of snow depth (H_2O mm) from air

3.1. Radiance of primary photons on soil surface

On the soil surface the intensity (strength and angular distribution) of the primary photons depends on photon source (emission rate) distribuiton $q(z)$, soil density $\rho(z)$ (we assume, these vary only with the depth z), and then on the mass attenuation coeffcient $\mu(z)$ in soil, Fig. 5. On the surface the intensity [16]

$$I = \frac{dN}{dA d\Omega} = \frac{1}{4\pi}\int_0^{\infty} q(z)dz \exp\left(-\int_0^{z} \mu\rho(z')dz'/\cos\varphi \right). \qquad (3)$$

For the homogeneous q, ρ and μ there is

$$I = \frac{q}{4\pi\mu\rho}\cos\varphi\,, \qquad (4)$$

Lambert's law. I think that

$$q(z) = q_0 - (q_0 - q_1)\exp(-z/\ell)\,, \qquad (5)$$

$q_1 < q_0$, can be a realistic model for Th, U and K sources in soil with litter on. Potassium is, however, also a fertilizer, and in fertilized soil its distribution is another. The deposition of radioactive Cs is mainly near soil surface.

Table 1 presents typical values for μ. Attenuation decreases with photon energy.

When the mass attenuation coeffcients are 4...5 10^{-3} m^2/kg for dry soil of 1500 kgm^{-3} then 4 % of photons penetrates 54…43 cm. For certain sources, e.g. $q_1 \approx q_0$ in (5), it is interesting to find $I(\varphi)$.

3.2. Airborne detection

The detector, Fig. 5, as mentioned, is often scintillator. NOHRSC [3] has in airplanes a broad area (51 x 41 cm^2) and 10.2 cm thick NaI(Tl) as the main instrument. The spectra of Fig. 1 and 2 are measured with the same type of detector. For the normalised responses of the 40 x 40 x 10 cm^3 detector [17], the fitting

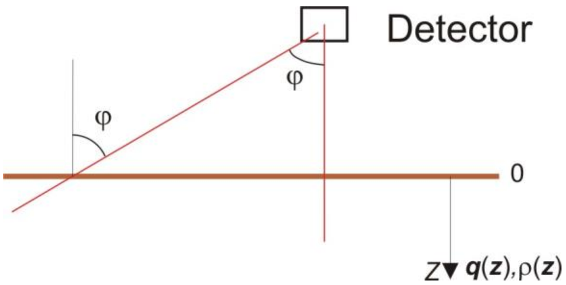

Fig. 5. Scheme of airborne measurement.

$$D = D_0 + D_1 \cos\varphi , \qquad (6)$$

where D_1/D_o = 0.44 for cesium, 0.59 for potassium and 0.72 for thorium, is a relatively good one. In snow measurement, see Fig. 6, the influences of the two terms of (6) do not differ very much.

Snow and air attenuate, and the counting rate of detector is calculated with

$$R = \int_h^\infty \frac{D(\varphi)I(\varphi)}{r^2} \exp(-\mu\rho r) 2\pi r dr, \qquad (7)$$

when the detector is at the height h. From (4) and (6) we get

$$R = [R_0 E_2(x) + R_1 E_3(x)]/(\mu_s \rho_s), \qquad (8)$$

where E_i are exponential integrals with the argument

$$x = \mu_a \rho_a h + (\mu_w \rho_w - \mu_a \rho_a) s .$$

s means water equivalent depth (e.g. H_2O mm) of snow cover. μ_s and ρ_s are soil values. The subscript a means air and w water, see table 1.

Table 1. Mass attenuation coefficients: μ_w (in water), μ_{ds} (in dry soil of mean earth crust composition, 0.14 weight% of H) and μ_a (in air, where water mole fraction is 0.0126), using compilations of Hubbell et al. [19] and Hubbell and Seltzer 1995 [20].

Window	Photon emitter	Energy keV	μ_w 10^{-3} m^2/kg	μ_{ds} 10^{-3} m^2/kg	μ_a 10^{-3} m^2/kg
Thorium	^{208}Tl	2614.5	4.27	3.87	3.85
Uranium	^{214}Bi	1764.5	5.28	4.74	4.76
Potassium	^{40}K	1460.8	5.83	5.22	5.25
Cesium	^{137}Cs	661.7	8.57	7.67	7.71

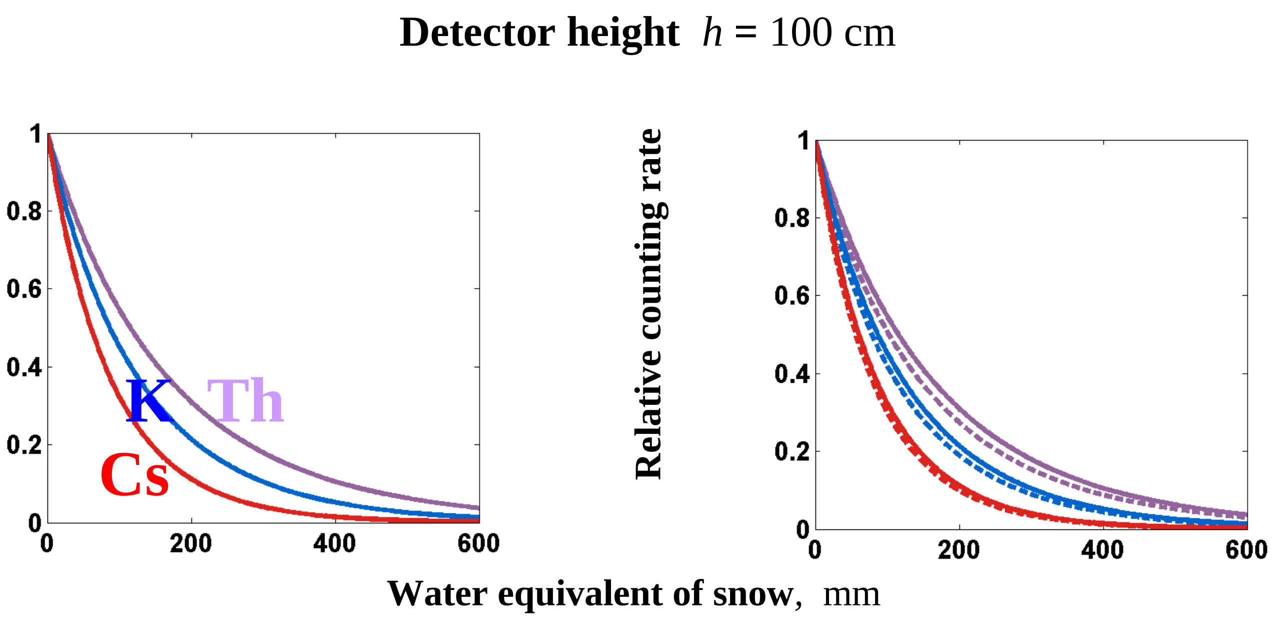

Fig. 6. Relative counting rates of thorium, potassium and cesium, left when $D = D_o \cos \theta$, and right the same and the result for $D = D_o$. The curves Th and K, when $q \neq q(z)$, the curve Cs, when a plane source at the depth 4 cm in soil.

4. Photon spectrum information

Th-photons can penetrate through thick snow layers. When the Cs activity is superior the Cs-photons gauge narrow layers most accurately.

In Fig. 3 the ratio M_2/M_1 and the values M_3 and M_2 may have useful information concerning e.g. soil moisture, cf. [2,23]. N_1, N_2 (and possible N_3) in Fig. 2 can have the same information.

5. The flight route

Earlier the flight route inaccuracies might be remarkable and cause errors. Today with the use of the satellite GPS (Global Position System) they can be minimised. The horizontal error of GPS [18] is almost always and easily below 5 m. Vehicle velocity and communications probably increase the error limits.

References

[1] Airborne Gamma Ray Spectrometer Surveying, International Atomic Energy Agency, Vienna,1991,Technical Reports Series No. 323.

[2] R.M. Kogan, I.M. Nazarov, D.S. Fridman, Gamma Spectrometry of Natural Environments and Formation, Jerusalem 1971.

[3] Airborne Gamma Survey Program, National Operational Hydrologic Remote Sensing Center, National Weather Service, NOAA http://www.nohrsc.nws.gov/snowsurvey/gammapage.html

[4] B.E. Goodison, A. Banga, R.A. Halliday, CWR Journal 9 (1984) no.1, 99. And E.L. Offenbacher, S.C. Colbeck, CRREL report 91-9 (1991).

[5] R. Kuittinen, M. Autti, J. Perälä, J. Vironmäki, Technical Research Centre of Finland 1985, Research reports 370 (in Finnish).

[6] A.E. Fritzsche, Publication No. NWS-8201, EG&G, Inc., Las Vegas, NV 1982, and Physics of the Airborne Gamma SWE Measurement, http://www.nohrsc.nws.gov/snowsurvey/physics.html

[7] R. Ribberfors, K.-F. Berggren, Phys. Rev. A 26 (1982) 3325.

[8] P.P. Kane, Radiat. Phys. Chem. 50 (1997) 31.

[9] J.H. Hubbell, Radiat. Phys. Chem. 50 (1997) 113.

[10] S. Kahane, in: Proc. 8th Int. Symposium on Radiation Physics (ISRP8), Prague, Czech 2000, Radiation Physics and Chemistry 61 (2001) 199.

[11] J.H. Hubbell, W.J. Veigele, E.A. Briggs, R.T. Brown, D.T. Cromer, R.J. Howerton, J. Phys. Chem. Ref. Data 4 (1975) 471.

[12] P.P. Kane, L. Kissel, R.H. Pratt ja S.C. Roy, Physics Reports (Review Section of Physics Letters) 140 (1986) 75-159.

[13] B.K. Chatterjee, S.C. Roy, J. Phys. Chem. Ref. Data 27 (1998) 1011.

[14] M. Schumacher, Radiation Physics and Chemistry 56 (1999) 101.

[15] P.B. Moon, Proc. Phys. Soc.A 63 (1950) 80.

[16] V.V. Larionov, Jadernaja Geologija i Geofizika, Gostoptehizdat 1963, Moscow.

[17] J.D. Allyson, D.C.W. Sanderson, J. Environ. Radioactivity 38 (1998) 259.

[18] D.L.Wilson, David L. Wilson's GPS Accuracy Web Page(2005), http://users.erols.com/dlwilson/gps.html

[19] J.H. Hubbell, H.A. Gimm, I. Øverbø, J. Phys. Chem. Ref. Data 9 (1980) 1023.

[20] J.H. Hubbell, S.M. Seltzer, U.S. Department of Commerce 1995, NISTR 5632.

[21] RESUME (Rapid Environmental Surveying Using Mobile Equipment) 1995. Airborne gamma ray spectrometer surveying, Nordic Nuclear Safety Research 1997, nks, Copenhagen.

[22] S. Kasi, in XXII Nordic Hydrological Conference, Røros, Norway 2002, NHP Report no. 47, 11, and Norja-2002.pdf (elisanet.fi)

[23] R.L. Grasty, J. Hydrology 55 (1982) 213.